

# Vehicle Mobility and Communication Channel Models for Realistic and Efficient Highway VANET Simulation

Nabeel Akhtar, *Member, IEEE*, Sinem Coleri Ergen, *Member, IEEE*, Ozgur Ozkasap, *Member, IEEE*

**Abstract**—Developing real-time safety and non-safety applications for vehicular ad hoc networks (VANETs) requires understanding the dynamics of the network topology characteristics since these dynamics determine both the performance of routing protocols and the feasibility of an application over VANET. Using various key metrics of interest including node degree, neighbor distribution, number of clusters and link duration, we provide a realistic analysis of the VANET topology characteristics over time and space for highway scenario. In this analysis, we integrate real-world road topology and real-time data extracted from the Freeway Performance Measurement System (PeMS) database into a microscopic mobility model to generate realistic traffic flows along the highway. Moreover, we use a more realistic, recently proposed, obstacle based channel model and compare the performance of this sophisticated model to the most commonly used and more simplistic channel models including unit disc and log-normal shadowing models. Our investigation on the key metrics reveals that both log-normal and unit disc models fail to provide realistic VANET topology characteristics. We therefore propose a matching mechanism to tune the parameters of the log-normal model according to the vehicle density and a correlation model to take into account the evolution of the link characteristics over time. The proposed method has been demonstrated to provide a good match with the computationally expensive and difficult to implement obstacle based model. The parameters of the proposed model have been validated to depend only on the vehicle traffic density based on the real data of four different highways in California.

**Index Terms**—vehicular ad hoc networks, simulation, channel model, mobility model

## I. INTRODUCTION

VANET is a promising Intelligent Transportation System (ITS) technology that offers many applications such as safety message dissemination [2], [3], [4], dynamic route planning [5], content distribution, gaming and entertainment [6]. The majority of the VANET research effort on protocol design has relied on simulations due to the prohibitive cost of deploying real world test-beds. Building a realistic simulation environment for VANET is therefore essential in judging the performance of the protocols proposed at various layers.

VANET simulation environment should be realistic requiring an accurate representation of the vehicular mobility and signal propagation among the vehicles, and also efficient necessitating a reasonable amount of simulation time. Realistic representation

Copyright (c) 2013 IEEE. Personal use of this material is permitted. However, permission to use this material for any other purposes must be obtained from the IEEE by sending a request to pubs-permissions@ieee.org. Nabeel Akhtar was with the Department of Computer Engineering, Koc University, 34450 Istanbul, Turkey. He is now with the Department of Computer Science, Boston University, MA, 02215 USA (e-mail: nabeel@bu.edu). Sinem Coleri Ergen is with the Department of Electrical and Electronics Engineering, Koc University, 34450 Istanbul, Turkey (e-mail: sergen@ku.edu.tr). Ozgur Ozkasap is with the Department of Computer Engineering, Koc University, 34450 Istanbul, Turkey (e-mail: oozkasap@ku.edu.tr). This work was supported by Turk Telekom under Grant Number 11315-07. Sinem Coleri Ergen also acknowledges support from Bilim Akademisi - The Science Academy, Turkey under the BAGEP program. An earlier version of this paper was presented at the IEEE Wireless Communications and Networking Conference (WCNC), April 2013 [1].

of the vehicle mobility requires using real-world road topology, accurate microscopic mobility modeling and real-data based traffic demand modeling whereas a realistic representation of the signal propagation among the vehicles requires reproducing the actual physical radio propagation process for a given environment. On the other hand, an efficient representation of the vehicle mobility and signal propagation model requires analyzing both the closeness to the realistic representations in terms of the key metrics summarizing the dynamics of the VANET topology in time and space, and the runtime of the simulations. As summarized in Table I, the literature on VANET topology characteristics focuses on realistic channel models tested on simplistic vehicle mobility models [7], [8], realistic mobility models without considering realistic signal propagation models [9], [11], [12], [14] or simplistic models for both vehicle mobility and communication channel [16], [17], [18], [19], [20], [21], [22]. Moreover, these models are often compared using classical metrics such as node degree, number of clusters, link duration and quality [16], [9], [17], [18] or related metrics such as packet loss probability and connectivity probability [19], [20], [7], [8], [22], [14]. They include only a small subset of important network-wide metrics summarizing the state of the network such as closeness centrality measuring how long it takes for the information to spread in a network, clustering coefficient giving information about the degree to which nodes tend to cluster and size of the largest group of connected vehicles in the network [17], [11], [12].

The goal of this paper is to analyze VANET topology characteristics on a large highway section by integrating realistic microscopic mobility traces generated using real-world road topology and real-data based traffic demand with realistic channel models taking into account the effect of vehicles on the received signal power. We compare the performance of this realistic scenario to the most commonly used and more simplistic channel models using various metrics of interest. The original contributions of the paper are listed as follows:

- We incorporate real-world road topology and real-time data from PeMS database [23] into the microscopic mobility model provided by Simulation of Urban Mobility (SUMO) [24]. PeMS database allows modeling realistic traffic flows on the highway by adjusting the parameters of the SUMO simulator to match the real data. This is the first work to analyze VANET topology characteristics over a large scale highway using an open source database for measuring vehicle traffic and speed.
- We incorporate more realistic recently proposed obstacle based channel model into the analysis of VANET topology characteristics and compare its performance to the most commonly used and more simplistic channel models including unit disc and log-normal shadow fading models. This is the first work to analyze the effect of using the obstacle based channel model on the VANET topology characteristics.
- Since it is hard to integrate the obstacle based model into

TABLE I: Related Work on Topology characteristics in VANETs

Ref	Topology	Channel Model	Vehicle Mobility	Database for Vehicle Mobility	Performance Criteria
[7]	Urban	Ray-tracing-derived models	Intelligent Driver Model on Manhattan-grid	No database used	Packet loss ratio, Average end-to-end delay
[8]	Urban	Two ray ground	Chain topology with nodes arranged at a regular interval	No database used	Packet loss distribution
[9]	Urban	Unit disc	Microscopic road traffic	TAPASCologne Dataset by German Aerospace Institute of Transportation Systems [10]	No. of clusters, Node degree
[11]	Urban	Unit disc	Microscopic road traffic	TAPASCologne Dataset by German Aerospace Institute of Transportation Systems [10]	Node degree, betweenness centrality, No. of clusters, Size of the largest cluster
[12]	Urban	Unit disc	Multi-agent microscopic traffic	Zurich traffic data used [13]	Node degree, Link duration, Diameter, Centrality, No. of clusters, Clustering coefficient
[14]	Urban, Highway, Suburban	Unit Disc, Two ray Model	Microscopic road traffic	DRIVE-IN Project [15]	Packet delivery rate, delay
[16]	Urban	Unit disc with LOS and NLOS	Cellular Automata based traffic mobility model on Manhattan-grid	No database used	Link duration, Link re-healing time
[17]	Mostly Urban	Unit disc	Constant Speed Motion, Manhattan, Fluid Traffic Motion, Intelligent Driver Model	No database used	Link duration, Node degree, No. of cluster, Cluster coefficient, Vehicular density distribution
[18]	Urban	Unit disc, Quasi-Unit disc, Log-normal shadowing	Microscopic road traffic	Map of city of Porto, no database for real traffic	Node degree, Link duration
[19]	Urban	Unit disc, Rayleigh Fading, Ricean Fading	Microscopic multi-model traffic	Map of Berlin and Frankfurt, no database for real traffic	Packet reception probability
[20]	Highway	Unit disc, Log-normal shadowing	Randomly generated	No database used	Access probability, Connectivity probability
[21]	Urban	Unit disc	Manhattan Model	No database used	Number of clusters
[22]	Urban	Log-normal shadowing, Multi-path fading	Microscopic road traffic	No database used	Packet delivery ratio

the modern simulators due to its high complexity and computational cost, we propose a matching mechanism to tune the parameters of the log-normal model according to the vehicle density and a correlation model to take into account the evolution of the link characteristics over time. We demonstrate the performance of the proposed method and validate the dependence of the parameters of the proposed model on the vehicle traffic density over four different highways in California. This is the first work to propose a method to adjust the parameters of the log-normal model and introduce time correlation depending on the vehicle density for more realistic and efficient VANET simulation.

- This is the first work to perform an extensive analysis of the VANET topology characteristics based on the realistic vehicle mobility and channel models. This analysis includes not only node degree, link duration, number of clusters but also neighbor distribution, closeness centrality, size of the largest cluster and clustering coefficient.

The rest of the paper is organized as follows. Section II discusses the related work on the vehicle mobility and communication channel models, and their usage in the analysis of VANET topology characteristics. Section III describes the generation of the realistic vehicle mobility using the PeMS database. Section IV defines different radio channel models including the unit disc, log-normal shadowing and obstacle based model. Section V describes the performance metrics used in the comparison of different channel models. Section VI introduces the matching mechanism used for tuning the parameters of the log-normal shadowing model. Simulation results and the validation of the proposed matching mechanism are presented in Sections VII and VIII respectively. Finally, concluding remarks and future work are given in Section IX.

## II. RELATED WORK

### A. Vehicle Mobility Models

Vehicular mobility simulators have been growing their complexity and features over time encompassing realistic road topologies and microscopic vehicular models, where each vehicle is represented as a separate entity and the behavior of vehicles depends on the neighboring vehicles [25]. SUMO [24], VISSIM [26], DIVERT [27], MMTS [28] are examples of such simulators.

The simulations are usually performed on small portions of a road with user generated traffic flows in these simulators and only recently have been extended to larger areas while incorporating a realistic model for the macroscopic mobility of the vehicles where the traffic flows are determined based on the real data. The real data used for this purpose in the recent studies on the analysis of the VANET topology characteristics in urban areas includes mobility traces gathered through various measurement campaigns [9], [11] and statistics performed by the urban planning and traffic engineering communities [12], [14]. None of these studies however analyze the VANET topology characteristics on a large-scale highway considering the real data based traffic demand of the vehicles.

### B. Communication Channel Models

Realistic representation of the signal propagation among vehicles requires reproducing the actual physical radio propagation process for a given environment based on the ray-tracing method [29], [7]. Ray-tracing approach generates the complex impulse response of the channel by determining possible paths or rays from the transmitter to the receiver according to the rules of geometrical optics. Such a model however is impractical since it requires a detailed description of the site-specific propagation environment.

Stochastic models on the other hand determine the physical parameters of the vehicular channel in a completely stochastic manner without presuming any underlying geometry [30]. The distance-dependent path loss, large scale and small scale fading distributions are the parameters to be estimated in these stochastic models as a result of extensive measurement campaigns. The path loss represents the local average received signal power relative to the transmit power as a function of the distance between the transmitter and receiver. The path loss exponent of  $n = 1.8 - 2.7$  was observed on highways in [31], [32], [33], [34]. The large-scale fading models the effect of the surrounding obstacles on the mean signal attenuation at a given distance. The surrounding obstacles may be mobile (e.g. other vehicles), or static (e.g. buildings in urban environments). Most of the channel modeling activities aim at averaging the additional attenuation due to these obstacles resulting in a log-normal distribution around the mean received signal power in urban areas [34], [35] and highways [35]. Although some of these models estimate different values for the variance of this large-scale fading distribution at high and low traffic densities [35], only recently a mechanism for incorporating the effect of the vehicles and static obstacles on the received signal power in highways has been proposed in [36] and [37] respectively. Finally, the small-scale fading models the effect of the reception of multiple replicas of the transmitted signal at the receiver. Various distributions have been proposed for small-scale fading including Rice [38], Nakagami [34] and Weibull [39], [35] distributions.

Although the signal propagation has great impact on the performance of the communication protocols, most of the recent work on the analysis of VANET topology characteristics are using unit disc as the signal propagation model, where the vehicles can communicate with each other if they are within a threshold distance and cannot communicate otherwise [16], [17], [9], [11], [18], [19], [20], [21], [12], [14]. Although recently such analysis employs more sophisticated stochastic signal propagation models including both large-scale fading [18], [20], [22] and small-scale fading [19], [22], none of these models incorporate the effect of the vehicles on the signal propagation.

### III. VEHICLE MOBILITY MODEL

Realistic representation of the vehicle mobility requires using accurate microscopic mobility modeling, real-world road topology and real-data based traffic demand modeling. The input and parameters of the microscopic mobility simulator are determined based on the real traffic flow and speed values measured by the road sensors deployed along the highway as detailed next.

#### A. Microscopic Mobility Modeling

SUMO [24] is used to simulate the microscopic mobility of the vehicles. SUMO, generated by the German Aerospace Center, is an open-source, space-continuous, discrete-time traffic simulator capable of modeling the behavior of individual drivers. The path of each driver is determined based on the origin/destination matrix provided as an input to the simulator. The movement of each driver is implemented using the surrounding vehicles via Krauss' car-following model that regulates its acceleration and Krajzewicz's lane-changing model that regulates its overtaking decisions [40]. The parameters of the simulator that determine the driver's acceleration and overtaking decisions include the distance to the leading vehicle, the traveling speed, the acceleration and deceleration profiles, and dimension of the vehicles.

#### B. Traffic Demand Modeling

PeMS collects historical and real-time data from highways in the State of California with the goal of providing a comprehensive assessment of highway performance [23]. PeMS was developed by the Department of Electrical Engineering and Computer Sciences at University of California Berkeley, in co-operation with the California Department of Transportation, California Partners for Advanced Transit and Highways, and Berkeley Transportation Systems. The flow and speed data are collected in real time from more than 25,000 individual road sensors located over all major metropolitan areas in the state of California. The sampling period of the flow and speed data ranges from 30 seconds to 5 minutes. We used road I-880S in Alameda County, Bay Area, California for our simulation. Fig. 1 shows the road sensors located on I-880S.

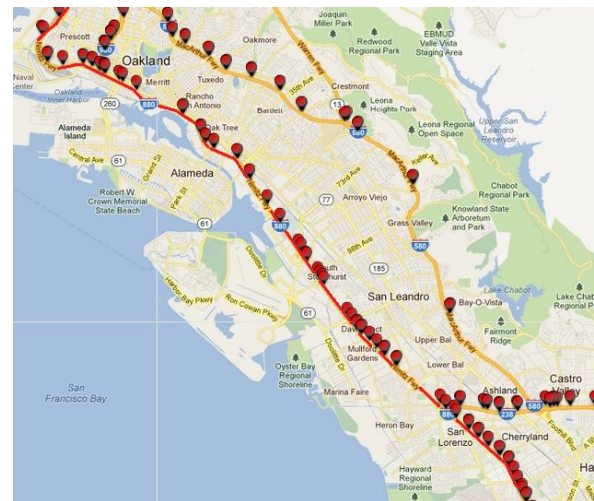


Fig. 1: Road sensors located on I-880S in Alameda County, Bay Area, California

#### C. Realistic Mobility Generation

The first step in generating the realistic mobility model is to determine the input of SUMO using the real-data based vehicular traffic flows over the road. The input of SUMO including the number of vehicles injected at each entry of the highway (the starting point of the vehicle) and the probability that each vehicle leaves the highway from the exits (destination of vehicles) is determined such that the expected number of vehicles passing through each road sensor location in the simulation closely matches the flow measured at that sensor on the actual highway. However, matching the traffic flow in the simulation to that of the PeMS database does not guarantee that the average speed of the vehicles in the simulation also matches the speed measured through PeMS. Therefore, the second step in generating realistic mobility model is to determine the parameters of SUMO such that the average speeds of the vehicles determined by the simulation and PeMS agree with each other. The parameters of SUMO adjusted for this purpose include the distance to the leading vehicle, the initial speed, the acceleration and deceleration profiles.

Figs. 2 and 3 show the standard deviation bars depicted around the mean of the flow and speed of the vehicles recorded from the simulation and PeMS database respectively. The data from 419 road sensors on highway I880-S, as shown in Fig. 1, are extracted for both high traffic density, i.e. at 18 : 00, and low traffic density, i.e.

at 01 : 00. Road sensors are on average 1.21 km apart from each other on the road. Vehicles are randomly and uniformly assigned to the lanes based on the PeMS measurement results aggregated over all lanes. As demonstrated in the figures, once the system stabilizes at around 10-th minute, both the average flow and speed from the simulation and PeMS database are consistent with each other.

Fig. 4 shows the cumulative distribution function (cdf) of the percentage error between the values extracted from the PeMS database and the values obtained from the simulation for the flow and speed of the vehicles at different vehicle traffic densities. The values are obtained over all the sensors at different time instants after the system stabilizes. We observe that for 80% of the values of the flow and speed, the error is less than 5% at low density traffic, and less than 12% at high density traffic. This demonstrates that the mobility of the vehicles in the simulation closely matches that in the PeMS database.

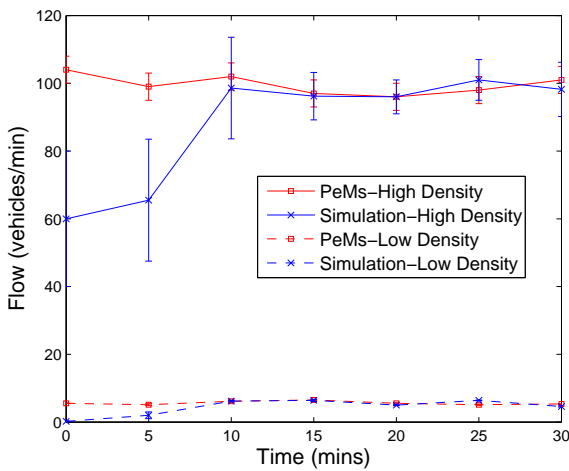


Fig. 2: Standard deviation bars depicted around the mean of the flow of the vehicles extracted from the PeMS database and obtained from the simulation at low and high vehicle traffic density.

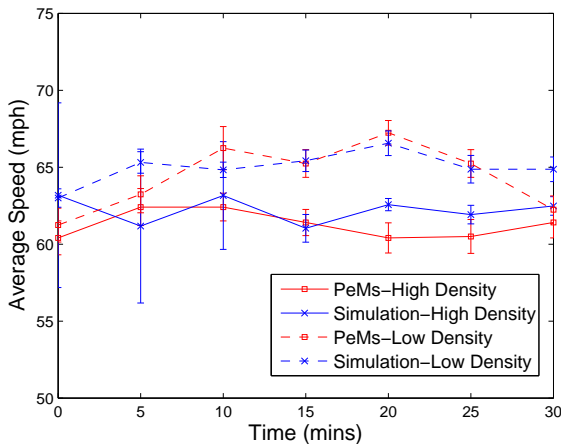


Fig. 3: Standard deviation bars depicted around the mean of the speed of the vehicles extracted from the PeMS database and obtained from the simulation at low and high vehicle traffic density.

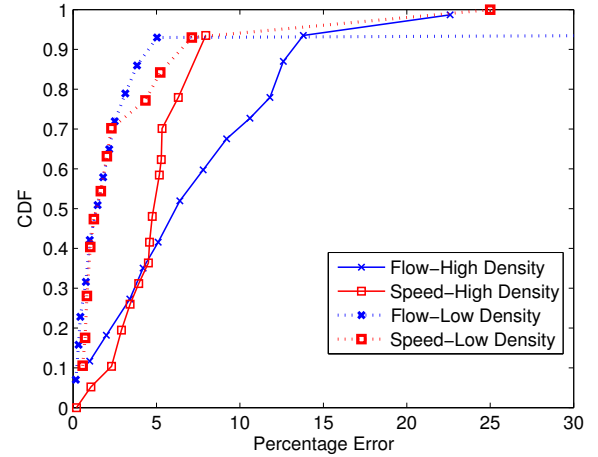


Fig. 4: Cdf of the percentage error between the values extracted from the PeMS database and the values obtained from the simulation for the flow and speed of the vehicles at low and high vehicle traffic density.

#### IV. VEHICULAR CHANNEL MODELS

In this section, we will first describe simplistic channel models including unit disc and log-normal shadowing models that are commonly used in the analysis of the VANET topology characteristics. We will then describe a recently proposed and more realistic obstacle based channel model that incorporates the effect of the moving obstacles (i.e. vehicles) on the received signal power due to their dominating influence as illustrated in [36]. The obstacle based model has not been used before in the VANET topology analysis.

##### A. Unit Disc Model

In the unit disc model, the vehicles can communicate with each other if they are within a threshold distance and cannot communicate otherwise. This model is widely used in the analysis of the VANET topology characteristics due to its simplicity [16], [17], [9], [18], [19], [20], [21], [12]. However, the sharp cut-off at the threshold distance not only fails to capture the random noise that can make even nearby nodes unreachable but also does not take into account the effect of the obstacles on the received signal strength.

##### B. Classical Log-Normal Shadowing Model

In the classical log-normal shadowing model, rather than calculating the additional attenuation due to each obstacle between the transmitter and receiver, the probabilistic distribution of the additional attenuation is modeled with a log-normal probability density function resulting in the following formulation for the received signal power [34], [35]:

$$P_{rx}(d) = P_0 - 10n \log_{10} \frac{d}{d_0} + N \quad (1)$$

where  $d$  is the distance between the transmitter and the receiver,  $d_0$  is the reference distance,  $P_{rx}(d)$  is the received signal power at distance  $d$  (in dBm),  $P_0$  is the received signal power at the reference distance  $d_0$  (in dBm),  $n$  is the path loss exponent and  $N$  is zero mean Gaussian random variable with variance  $\sigma^2$ . A vehicle can communicate with another vehicle if  $P_{rx}$  is greater than a certain

threshold value [20]. Note that the log-normal shadowing model reduces to the unit disc model if  $\sigma = 0$ . The parameters of the log-normal model is chosen such that the mean transmission range is equal to the threshold distance in the unit disc model to have a fair comparison. The parameters  $n$  and  $\sigma$  of the model are chosen based on the channel measurement results reported in [31], [32], [33], [34], [35]:  $n = 2.5$ ,  $\sigma = 5.5$  dB.

### C. Obstacle based Channel Model

In the obstacle based channel models, algorithms to incorporate the effect of the surrounding obstacles such as other vehicles, walls and buildings on the received signal strength have been proposed [35], [36] rather than modeling the average additional attenuation due to these obstacles by a stochastic large-scale fading model. Usually there are a few buildings around the highway, mostly far from the vehicles. That is why, in this study, we only consider the impact of the surrounding vehicles as obstacles. Since the additional obstacles can only further reduce the probability of the line-of-sight (LOS) between the transmitter and receiver vehicles, this approach gives a best case analysis for the probability of LOS as stated in [36].

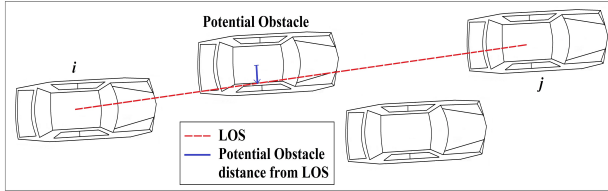


Fig. 5: Determining the vehicles potentially obstructing the LOS between vehicles  $i$  and  $j$

The algorithm proposed and validated in [36] is implemented for calculating the additional attenuation due to the vehicles. This algorithm consists of three main parts: First, the vehicles potentially obstructing the LOS between the transmitter vehicle  $i$  and receiver vehicle  $j$  are determined ( $getPotentialObs(i, j)$ ): If the distance from the center of the vehicle to the LOS line between vehicles  $i$  and  $j$  is less than half the width of the vehicle, the vehicle is considered as a potential obstacle as illustrated in Fig. 5 (Line 1 of Algorithm 1).

**Algorithm 1** Obstacle Based Model: Calculation of the additional attenuation between vehicles  $i$  and  $j$  due to surrounding vehicles as obstacles

```

1:  $[PotentialObs] = getPotentialObs(i, j)$ 
2: if  $size([PotentialObs]) \neq 0$  then
3:    $[ObsVeh] = getLOSobs([PotentialObs])$ 
4:   if  $size([ObsVeh]) \neq 0$  then
5:      $addAttenuation = calAttenuation([ObsVeh])$ 
6:   else
7:      $addAttenuation = 0$ 
8:   end if
9: else
10:   $addAttenuation = 0$ 
11: end if

```

Second, the vehicles that obstruct the LOS between vehicles  $i$  and  $j$  are chosen from the set of the potential obstructing vehicles identified in the previous step ( $getLOSobs([PotentialObs])$ ): From the electromagnetic wave propagation perspective, the LOS is not guaranteed with the existence of the visual sight line between

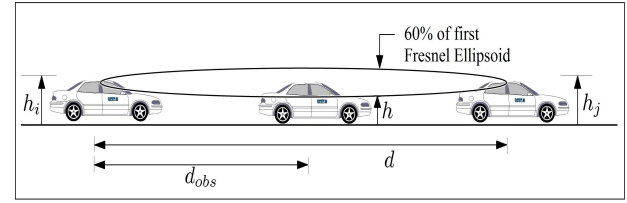


Fig. 6: Determining the vehicles that obstruct the LOS between vehicles  $i$  and  $j$  (For simplicity, vehicle antenna heights ( $h_a$ ) are not shown).

the transmitter and receiver. Any vehicle that obstructs the Fresnel ellipsoid might affect the transmitted signal. The effective height of the LOS line that connects vehicles  $i$  and  $j$  at the potential obstacle vehicle location when we use the first Fresnel ellipsoid is given by

$$h = (h_j - h_i) \frac{d_{obs}}{d} + h_i - 0.6r_f + h_a \quad (2)$$

where  $h_i$  and  $h_j$  are the heights of the transmitter vehicle  $i$  and receiver vehicle  $j$  respectively,  $d_{obs}$  is the distance between the transmitter and the obstacle,  $d$  is the distance between the transmitter and receiver,  $h_a$  is the height of the vehicle antennas, and  $r_f$  is the radius for the first Fresnel zone ellipsoid which is given by

$$r_f = \sqrt{\frac{\lambda d_{obs}(d - d_{obs})}{d}} \quad (3)$$

with  $\lambda$  denoting the wavelength. Fig. 6 illustrates these parameters. If the height of each potentially obstructing vehicle is known beforehand, the vehicle will obstruct the LOS between the transmitter and receiver if  $h$  is greater than its height. Based on the assumption that the vehicle heights follow a normal distribution as also assumed in [36], the probability of the LOS for the link between vehicles  $i$  and  $j$  is calculated as

$$\Pr(LOS|h_i, h_j) = 1 - Q\left(\frac{h - \mu_h}{\sigma_h}\right) \quad (4)$$

where  $\mu_h$  and  $\sigma_h$  are the mean and standard deviation of the height of the obstacle vehicle (Line 3 of Algorithm 1).

Third, the additional attenuation in the received signal power is calculated for the LOS obstructing vehicles determined in the previous step ( $calAttenuation([ObsVehicles])$ ). The existing models to calculate the attenuation are empirical and vary from optimistic [41] to pessimistic approximations [42], [43]. To calculate the additional attenuation, we used the ITU-R method based on the multiple knife edge model [44] as suggested in [36]. In this model, a complete profile is created for all the LOS obstructing vehicles, and the signal attenuation is calculated based on the vehicle height, distance from the transmitting vehicle, wavelength of electromagnetic waves and position of the vehicles (Line 5 of Algorithm 1).

## V. PERFORMANCE METRICS

The performance metrics are used in the comparison of different signal propagation models. For the formal definition of these metrics, we represent the vehicular network topology at time  $t$  by a graph  $G(t) = (V(t), E(t))$  where  $V(t)$  is the set of vehicles and  $E(t) \subset V(t) \times V(t)$  are the directed edges representing the wireless communication links between the vehicles.

### A. Neighbor Distance Distribution

Neighbor distance distribution is defined as the distribution of the distance of the neighbors of the vehicles in the network. Let us denote the set of neighbors at distance  $p$  away from vehicle  $i$  at time  $t$  by  $N_i(t, p)$  such that  $N_i(t, p) = \{j | (i, j) \in E(t), d_{ij} = p\}$  where  $d_{ij}$  is the distance between vehicles  $i$  and  $j$ . The neighbor distance distribution as a function of the distance  $p$  denoted by  $f(p)$  is then formulated as  $f(p) = \frac{1}{T} \sum_{t=1}^T \frac{1}{|V(t)|} \sum_{i=1}^{|V(t)|} |N_i(t, p)|$  where  $|V(t)|$  is the total number of the vehicles in the network at time  $t$  and  $T$  is the total simulation time. Neighbor distance distribution measures the distribution of the communicating vehicles over space.

### B. Node Degree

Node degree of a vehicle is defined as the number of the neighboring vehicles it can communicate with. Let us denote the set of neighbors of vehicle  $i$  at time  $t$  by  $N_i(t)$  such that  $N_i(t) = \{j | (i, j) \in E(t)\}$ . Note that  $N_i(t) = \int_0^\infty N_i(t, p) dp$ . The degree of vehicle  $i$  is then formulated as  $deg_i(t) = |N_i(t)|$ . Node degree measures the density of the network from the physical connectivity point of view.

### C. Link Duration

Link duration is defined as the time span between the instants at which the communication link between two vehicles is established and lost. Let us denote the times when the link from vehicle  $i$  to vehicle  $j$  is established and broken by  $t_0$  and  $t_f$  respectively such that  $(i, j) \notin E(t_0 - \epsilon)$ ,  $(i, j) \notin E(t_f + \epsilon)$  for arbitrarily small  $\epsilon > 0$  and  $(i, j) \in E(\tau)$ ,  $\forall \tau \in [t_0, t_f]$ . Then the duration of the link from vehicle  $i$  to vehicle  $j$  denoted by  $l_{ij}$  is formulated as  $l_{ij} = t_f - t_0$ . Link duration measures the stability of a connection over time.

### D. Number of Clusters

Number of clusters is defined as the number of co-existent, non-connected groups of vehicles at a given instant. We define cluster as a connected group of vehicles within which there exists a path between any pair of nodes. Formally, let us denote the existence of a path from vehicle  $i$  to vehicle  $j$  at time  $t$  by the binary variable  $p_{ij}(t)$  such that  $p_{ij}(t)$  takes value 1 if  $(i, j) \in E(t)$  or there exists  $k$  for which  $(i, k) \in E(t)$  and  $p_{kj}(t) = 1$ , and value 0 otherwise. Let us also define the cluster in which vehicle  $i$  is located at time  $t$  as  $C_i(t) = i \cup \{j | p_{ij}(t) = 1, p_{ji}(t) = 1\}$ . The set of unique clusters in the network at time  $t$  is formulated as

$$C(t) = \{C_i(t) | C_i(t) \cap C_k(t) = \emptyset, \forall k \in [1, i-1], \forall i \in V(t)\} \quad (5)$$

The number of clusters denoted by  $c(t)$  is then equal to  $|C(t)|$ . Number of clusters measures the degree of fragmentation in the network in terms of the number of mutually isolated groups of vehicles.

### E. Size of the Largest Cluster

Size of the largest cluster is defined as the number of vehicles in the largest cluster of the vehicular network. Formally, the size of the largest cluster denoted by  $c_{\max}(t)$  is formulated as  $c_{\max}(t) = \max_{i \in V(t)} |C_i(t)|$ .

### F. Clustering coefficient

Clustering coefficient is defined as the ratio of the number of the links within a cluster to the maximum number of the links that could exist within a cluster. Let us denote the set of the links within cluster  $C_i(t)$  by  $E_{C_i}(t) = \{(i, j) | (i, j) \in E(t); i, j \in C_i(t)\}$ . The clustering coefficient of the same cluster denoted by  $k_{C_i}(t)$  is then formulated as

$$k_{C_i}(t) = \frac{|E_{C_i}(t)|}{|C_i(t)|(|C_i(t)| - 1)} \quad (6)$$

Clustering coefficient measures the degree of connectivity of the vehicles within a cluster. Note that the clustering coefficient has a maximum value 1 if the cluster is a clique.

### G. Closeness Centrality

Closeness centrality of a vehicle is defined as the inverse of the sum of the number of hops to all other nodes that are reachable from that vehicle. Formally, the closeness centrality of vehicle  $i$  is defined for every  $i$  such that there exists at least one reachable vehicle from vehicle  $i$ , i.e.  $\{j | p_{ij}(t) = 1, j \neq i\} \neq \emptyset$ , denoted by  $CC_i(t)$  and formulated as

$$CC_i(t) = \frac{1}{\sum_{\{j | p_{ij}(t)=1\}} h_{ij}} \quad (7)$$

where  $h_{ij}$  is the number of hops in the shortest path from vehicle  $i$  to vehicle  $j$ . Closeness centrality measures how long it will take information to spread from a given vehicle to other reachable vehicles in the network.

## VI. MATCHED LOG-NORMAL SHADOWING MODEL

The classical log-normal shadowing model is based on specifying the probabilistic distribution of the additional attenuation due to the vehicles instead of calculating the attenuation due to each vehicle acting as obstacle separately. Since the decision for the existence of the communication link between every pair of vehicles requires specifying the value of a random variable only, independent of the number of the vehicles, the runtime of the simulations using this model is reasonable at  $O(|V(t)|^2)$  at time  $t$ . However, the parameters of this model, including the path loss exponent and the standard deviation of the Gaussian distribution, are fixed independent of the density of the surrounding vehicles leading to unrealistic simulations.

The obstacle based channel model, on the other hand, incorporates the effect of each vehicle on the received signal strength separately. Since the decision for the existence of the communication link between every pair of vehicles requires determining the effect of every other vehicle on the received signal strength, the accurate representation of the channel comes at the cost of high runtime complexity at  $O(|V(t)|^3)$  at time  $t$ . This prevents the integration of this model into the network simulators.

Fig. 7 shows the average runtime of the analysis of the performance metrics based on the 1800 sec simulation of the scenario where the vehicles are generated using the real data at different traffic densities and communicating with mean transmission range of 500 m under unit disc, classical log-normal and obstacle based channel models denoted by *Unit*, *Log<sub>C</sub>* and *Obs* respectively. We observe that the average runtime of the obstacle based model is about 100 times more than that of the unit disc and classical log-normal models increasing at a much higher rate as a function of the vehicle traffic density.

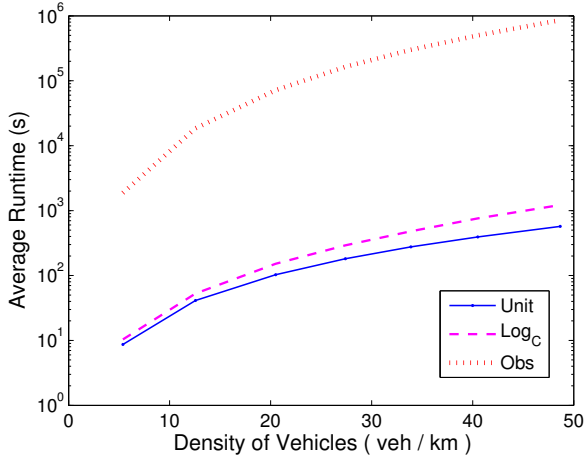


Fig. 7: Average runtime of the analysis of the performance metrics based on the 1800 sec simulation of the scenario where the vehicles are generated using the real data at different traffic densities and communicating with mean transmission range of 500 m under different channel models.

In this section, we propose a matching mechanism to tune the parameters of the log-normal model such that the performance metrics summarizing the link characteristics over space agree with those of the obstacle based model (Section VI-A). We also introduce a correlation model to take into account the evolution of the link characteristics over time and propose a mechanism to tune the parameters of this model to match the performance metrics summarizing the time characteristics of the links to those of the obstacle based model (Section VI-B). The resulting matched log-normal model provides performance close to that of the obstacle based model at much lower computational cost and implementation complexity allowing its integration into the network simulators. The reason for choosing log-normal channel model in the matching mechanism is that log-normal channel model is commonly used, supported by the channel measurement results reported in [31], [32], [33], [34], [35] and allows adjusting the probabilistic behavior of the communication links over both space and time.

---

**Algorithm 2** Matching Parameters of Log-normal Shadowing Model

---

**Input:**  $nValues, \sigmaValues$

**Output:**  $n_m, \sigma_m$

---

```

1:  $NDObs = cdfND(ObsModel);$ 
2:  $Error_{min} = \infty;$ 
3: for all  $nValues$  do
4:   for all  $\sigmaValues$  do
5:      $NDLog = cdfND(LogModel, n, \sigma);$ 
6:      $Error = Diff(NDObs, NDLog);$ 
7:     if  $Error < Error_{min}$  then
8:        $Error_{min} = Error;$ 
9:        $n_m = n;$ 
10:       $\sigma_m = \sigma;$ 
11:     end if
12:   end for
13: end for

```

---

**A. Matching Parameters of Log-normal Model**

The parameters of the log-normal model that need to be matched for the spatial evolution of the link characteristics include the path loss exponent and standard deviation of the Gaussian random variable.

Our matching algorithm to tune these path loss exponent and standard deviation parameters is given in Algorithm 2. The inputs of the algorithm are the set of possible values for the path loss exponent and standard deviation denoted by  $nValues$  and  $\sigmaValues$  respectively.  $nValues$  and  $\sigmaValues$  are chosen in the range of [1.5–5] and [5–20] respectively based on the channel measurement results reported in [31], [32], [33], [34], [35]. The outputs of the algorithm are the values for the path loss exponent and standard deviation that provide the best match to the obstacle based model denoted by  $n_m$  and  $\sigma_m$  respectively.

The algorithm starts by extracting the cdf of the node degree metric for the obstacle based model by using function  $cdfND$  with the parameter  $ObsModel$  representing obstacle based model and storing the resulting cdf in the variable  $NDObs$ , and initializing minimum error to infinity by using variable  $Error_{min}$  (Lines 1–2). The algorithm then computes the cdf of the node degree metric of the log-normal model, represented by  $LogModel$ , and storing the resulting cdf in the variable  $NDLog$  for every possible value of the path loss exponent and standard deviation, stored in the variables  $n$  and  $\sigma$  respectively in each iteration (Lines 3–5). The difference between the cdf of the obstacle based and log-normal models is then calculated by using Kolmogorov-Smirnov statistic defined as  $sup_x |NDObs(x) - NDLog(x)|$  in the function called  $Diff$  (Line 6). The values of the path loss exponent and standard deviation that provide the minimum difference are then selected to provide the best match to the obstacle based model (Lines 7–11). If the value of  $Error_{min}$  is not low enough at the end of the algorithm, the matching process can be repeated with an extended set of values for  $nValues$  and  $\sigmaValues$  at the input. However, the proposed initial ranges for the path loss exponent and standard deviation parameters always provided low  $Error_{min}$  value in the extensive simulations given in Section VII.

The reason for choosing the cdf of the node degree in the matching algorithm is that node degree is a measure of the spatial distribution of the nodes in the network. The above process is repeated for the neighbor distance distribution metric to validate the values  $n_m$  and  $\sigma_m$ . To obtain common values for  $n_m$  and  $\sigma_m$  from the matching algorithm of both the node degree and neighbor distance distribution metrics, we have determined all the values of  $n$  and  $\sigma$  that achieve  $Error$  within the 5% of the  $Error_{min}$  of both metrics. Then out of all the  $n$  and  $\sigma$  values that overlap, the ones corresponding to the minimum error of the node degree metric are assigned to  $n_m$  and  $\sigma_m$  respectively. If there is no overlapping  $n$  and  $\sigma$  values, then the percentage of getting closer to  $Error_{min}$  can be increased. However, such overlapping values were always found in the extensive simulations given in Section VII. The matching of the remaining performance metrics are justified in Section VII. Similarly, if it is important for an application to match another metric that is a measure of the spatial distribution of the nodes more closely than node degree, it can be used in the matching algorithm. However, the matching of the remaining performance metrics should again be justified in that case.

## B. Matching Time Correlation

The instances of the Gaussian variable used in the classical log-normal model are calculated independently at each time step of the simulation resulting in zero correlation of the link characteristics over time. The obstacle based model on the other hand provides the time correlation of the link characteristics implicitly due to the slow changes in the relative locations of the obstacles between the transmitter and receiver vehicles. We therefore extend the classical log-normal model to include a correlation model taking into account the temporal evolution of the link characteristics.

We used Gudmunson model with exponential correlation function for this work [45]. This model has been previously used for spatially correlated processes [46], [47]. However, as described in [48], this model can also be used for time correlation. The model describes the correlation of the shadowing process at time difference  $\Delta t$  by

$$Corr(\Delta t) = \sigma^2 \cdot \exp(-\alpha \Delta t)$$

where  $\sigma$  is the standard deviation of the Gaussian variable at each time instant, and  $\alpha$  is the correlation factor.

---

### Algorithm 3 Matching Correlation Factor for Log-normal Shadowing Model

---

**Input:**  $n_m, \sigma_m, \alpha Values$

**Output:**  $\alpha_m$

---

```

1:  $LDObs = cdfLD(ObsModel);$ 
2:  $Error_{min} = \infty;$ 
3: for all  $\alpha Values$  do
4:    $LDLog = cdfLD(LogModel, n_m, \sigma_m, \alpha)$ 
5:    $Error = Diff(LDObs, LDLog)$ 
6:   if  $Error < Error_{min}$  then
7:      $Error_{min} = Error;$ 
8:      $\alpha_m = \alpha;$ 
9:   end if
10: end for

```

---

The matching algorithm to tune the value of the correlation factor is given in Algorithm 3. The inputs of the algorithm are the values of the path loss exponent and standard deviation providing the best match with the spatial link characteristics of the obstacle based model, i.e.  $n_m$  and  $\sigma_m$  respectively, and the set of possible values for the correlation factor denoted by  $\alpha Values$ .  $\alpha Values$  are chosen in the range of  $[0 - 2]$  based on the correlation coefficient values used in [45], [46], [47], [48]. The output of the algorithm is the value of the correlation factor that provides the best match with the temporal link characteristics of the obstacle based model denoted by  $\alpha_m$ .

The algorithm starts by determining the cdf of the link duration metric for the obstacle based model by using function  $cdfLD$  and storing the resulting cdf in the variable  $LDObs$ , and initializing minimum error to infinity (Lines 1 – 2). The reason for choosing the cdf of the link duration is that link duration is a measure of the stability of the links over time. The algorithm continues by computing the cdf of the link duration metric of the log-normal model with the matched parameters  $n_m$  and  $\sigma_m$ , and every possible value of the correlation factor stored in the variable  $\alpha$ , and storing the resulting cdf in the variable  $LDLog$  in each iteration (Lines 3 – 4). The difference between the cdf of the link duration of the log-normal and obstacle based models is then calculated by using Kolmogorov-Smirnov statistics in the function  $Diff$  (Line 5). The value of the correlation factor giving the minimum difference is

selected as the best match value  $\sigma_m$  (Lines 6 – 9). If the value of  $Error_{min}$  is not low enough at the end of the algorithm, the matching process can be repeated with an extended set of values for  $\alpha Values$  at the input. However, the proposed initial range for the correlation factor always provided low  $Error_{min}$  value in the extensive simulations given in Section VII.

## VII. SIMULATION RESULTS

The goal of the simulations is to compare the effect of different channel models including the unit disc, classical log-normal fading, obstacle based and matched log-normal channel models on the topology characteristics of VANET located on a large-scale highway by comparing the node degree, neighbor distance distribution, link duration, closeness centrality, number of clusters, size of the largest cluster and clustering coefficient metrics of the resulting communication graphs as explained in Section V. Although we provide the cdf of the absolute values of all the metrics, we focus on the closeness of different channel models in terms of these metrics. A certain discrepancy between the obstacle based model and one of the unit disc, classical log-normal fading and matched log-normal channel models in some of the metrics may be tolerable for some vehicle applications.

In all the figures in this section, the unit disc, classical log-normal, matched log-normal and obstacle based channel models are denoted by  $Unit$ ,  $Log_C$ ,  $Log_M$  and  $Obs$  respectively, and  $R$  refers to the mean transmission range of the vehicles, which is achieved by adjusting the transmission power in all the channel models.

The topology of the VANET is obtained by using the accurate microscopic mobility modeling of SUMO while determining its input and parameters based on the PeMS database as explained and validated in detail in Section III. The flow and speed data of 419 road sensors on highway I880-S as shown in Fig. 1 at both high traffic density, i.e. 121 vehicles/km at 18 : 00, and low traffic density, i.e. 11 vehicles/km at 01 : 00, are used for this purpose. The performance metrics are extracted after the system stabilizes around the 10-th minute as illustrated in Figs. 2 and 3. The vehicle mobility output of SUMO is then input to MATLAB where the channel models are implemented and the performance metrics are derived and plotted. The datasets can be found in [49].

Figs. 8 a) and b) show the neighbor distance distribution for low and high density networks respectively. Note that the distance in the neighbor distance distribution is quantized into bins of 25 m in this figure. The matched log-normal model follows the obstacle based model closely. The difference between the obstacle based model and commonly used unit disc and classical log-normal fading models on the other hand increases as the vehicle density increases and the transmission range becomes greater than 100 m. To elaborate on the effect of this different behavior on the performance metrics, we therefore plot the rest of the graphs at transmission ranges of 100 m and 500 m for both low and high vehicle traffic densities.

Figs. 9 a) and b) show the cdf of the node degree metric for different channel models and transmission ranges in low and high density network respectively. The cdf of the node degree shows the total number of the vehicles each vehicle can communicate with, which is summed over all the distances but considering every vehicle separately over time. Neighbor distance distribution on the other hand differentiates the number of vehicles each vehicle can communicate with over distance but averages these values over time and all the vehicles in the network. Therefore, node degree and neighbor distance distribution together determine the neighborhood

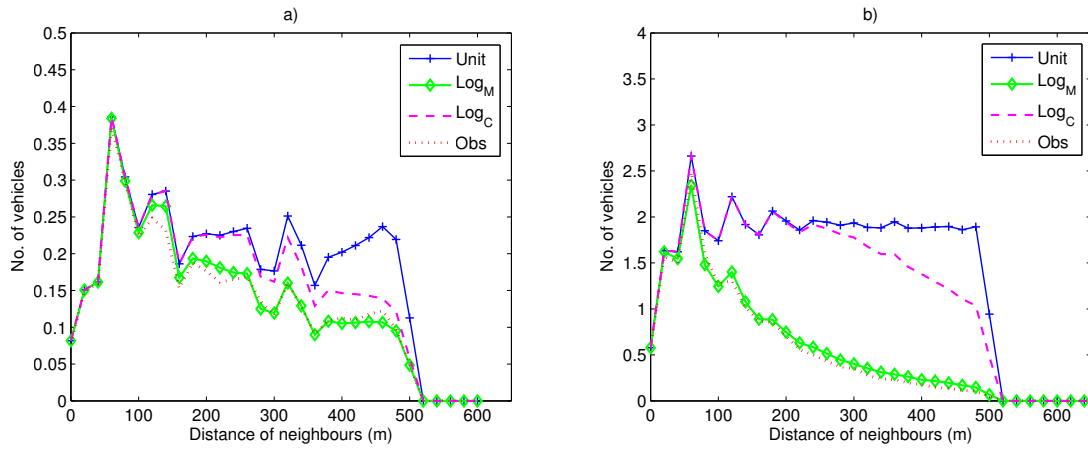


Fig. 8: Neighbor distance distribution for a) low density and b) high density networks at 500 m transmission range.

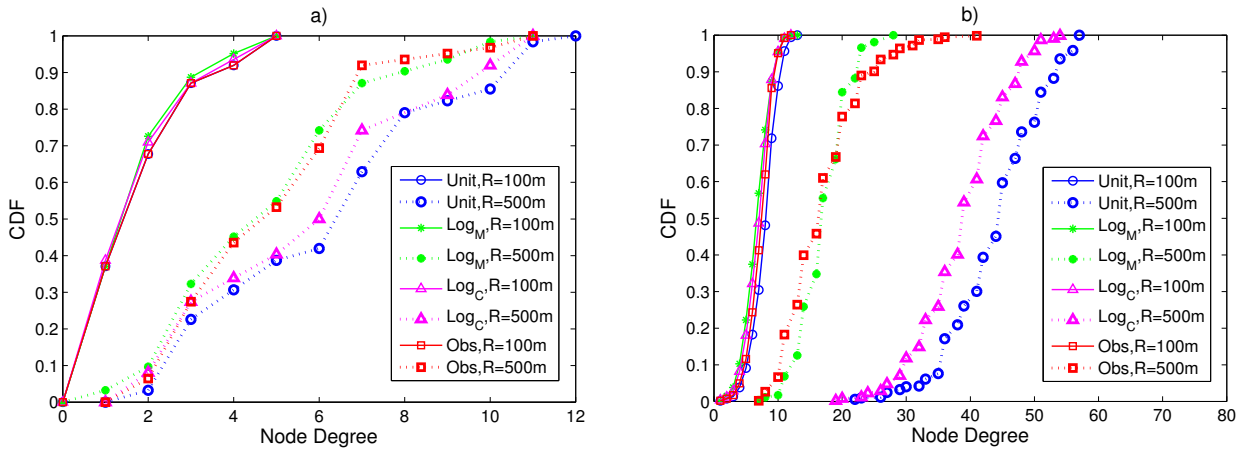


Fig. 9: Cdf of the node degree metric for different channel models and transmission ranges in a) low density and b) high density networks

of each vehicle across distance and time. All channel models generate the node degree distribution very close to each other at low transmission range for both low and high density networks. As the transmission range and the density of the network increase, the discrepancy between the obstacle based model and unit disc and classical log-normal fading models increases as expected from the difference observed in the neighbor distance distribution. The matched log-normal model on the other hand still agrees with the obstacle based model for all scenarios.

Figs. 10 a) and b) show the cdf of the link duration metric for different channel models and transmission ranges in low and high density network respectively. The link duration of the matched log-normal model again is very close to that of the obstacle based model for all scenarios. Besides, the link duration for the obstacle based model is smaller than that of the unit disc model and larger than that of the log-normal model. The main reason is that the nodes can always communicate with each other within a threshold distance for the unit disc model creating high correlation of the connectivity behavior over time so much higher link duration. On the other hand, the connections between the vehicles are determined probabilistically for the log-normal model where the probability is chosen independently in each step creating low correlation of the connectivity behavior so much lower link duration. The link duration for the obstacle based model is closer to the unit disc model at low transmission range and closer to the log-normal model at high transmission range meaning the correlation of the

connectivity behavior decreases as the transmission range increases in the obstacle based model. Moreover, we observe that the behavior of the link duration as a function of the transmission range does not agree for the unit disc and obstacle based models. As the transmission range increases from 100 m to 500 m, the link duration decreases under the obstacle based model whereas it increases under the unit disc model. The main reason for this behavior is that with the increase in the transmission range, the vehicles stay as neighbors for longer time under the unit disc model whereas the number of vehicles and their probability of acting as obstacles increases at larger transmission range under the obstacle based model. Furthermore, we notice that the link duration under the obstacle based model decreases as the vehicle traffic density increases due to the increasing probability of the vehicles acting as obstacles at higher density.

Fig. 11 shows the cdf of the number of clusters metric for different channel models and transmission ranges in low density network. Since the number of clusters is very low for high density networks when the transmission range is between 100 m and 500 m, we did not include a separate graph for the high density network. The distributions of the number of clusters based on the unit disc and obstacle based models are very close to each other. The main reason for this similarity even at different transmission ranges is that the vehicle which acts as an obstacle between two vehicles also acts at the same time as a bridge between them resulting in an indirect connection through the obstructing vehicle. The vehicles

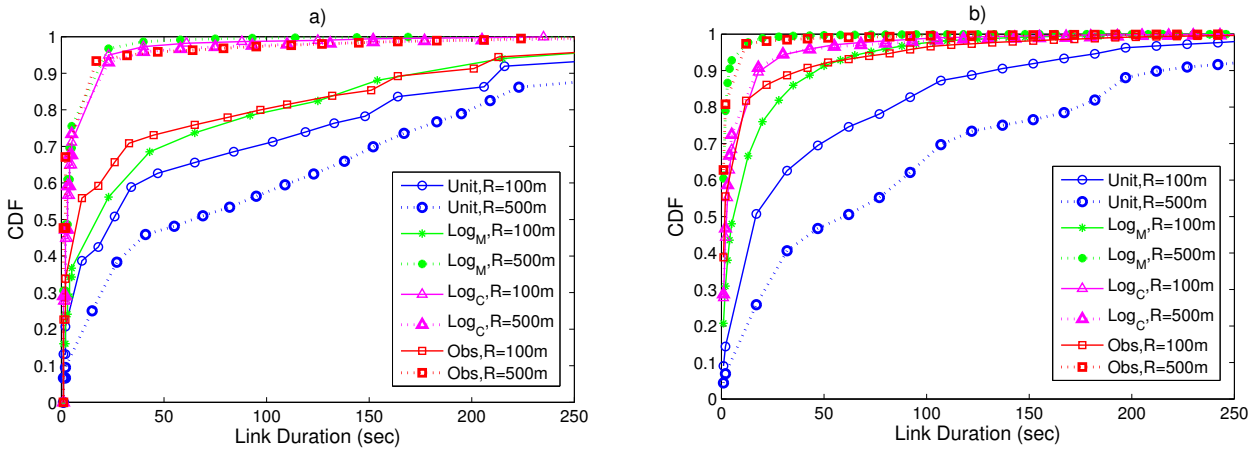


Fig. 10: Cdf of the link duration metric for different channel models and transmission ranges in a) low density and b) high density networks

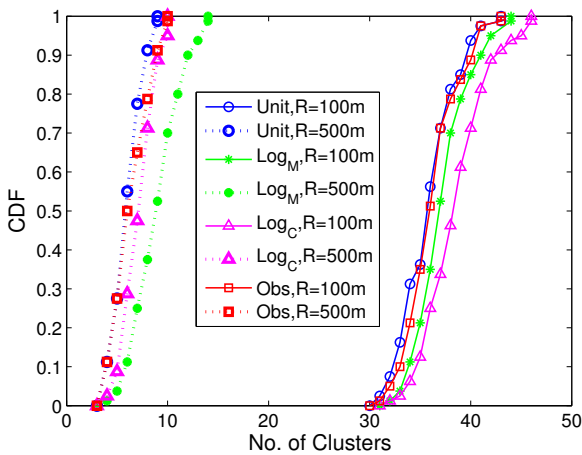


Fig. 11: Cdf of the number of clusters metric for different channel models and transmission ranges in low density network

are directly connected when unit-disc model is used whereas they are connected through the obstacles in the obstacle based model, resulting in the same number of vehicles within clusters. The number of clusters of the matched log-normal model is still close to that of the obstacle based model but slightly worse than that of the unit disc and classical log-normal models. This small difference mainly results from not including the spatial correlation of the Gaussian variables in the log-normal model. Obstacle based model implicitly includes the correlation among the links closer to each other in space due to the inclusion of the obstacles whereas the random variables generated for each link in the matched log-normal model are chosen independently over space.

Figs. 12 a) and b) show the cdf of the size of the largest cluster for different channel models and transmission ranges in low and high density network respectively. The size of the largest cluster for unit disc and matched log-normal model is very close to that of the obstacle based model whereas the largest cluster size is very different for classical log-normal and obstacle based models. This demonstrates the unsuitability of the classical log-normal model formulated with the same parameters at different network densities and the benefit of the additional matching process included in the matched log-normal model, .

Figs. 13 a) and b) show the cdf of the clustering coefficient metric for different channel models and transmission ranges in low and high density network respectively. Although the unit disc and obstacle based models agree with each other in the number of clusters and size of the largest cluster metrics, we observe that their performance is very different when the clustering coefficient is considered. The reason is that the clustering coefficient provides the degree of the connectivity of the vehicles within a cluster, which differentiates between the direct connectivity and the connection through the obstacles unlike the number of clusters and size of the largest cluster metrics. On the other hand, the matched log-normal model provides clustering coefficient values much closer to those of the obstacle based model than unit disc and classical log-normal models in most scenarios. The slight difference between the matched log-normal and obstacle based models again mainly comes from not including the spatial correlation of the Gaussian variables in the log-normal model.

Figs. 14 a) and b) show the cdf of the closeness centrality metric for different channel models and transmission ranges in low and high density network respectively. Similarly, the matched log-normal model provides very close performance to that of the obstacle based model unlike the classical log-normal model.

## VIII. VALIDATION OF RESULTS

Section VII demonstrates that the calibration of the path loss exponent, standard deviation and correlation factor parameters in the matched log-normal model achieves very close performance to the obstacle based model in terms of several metrics at different traffic densities. This section aims to validate the dependence of the values of these parameters on the vehicle traffic density only, across different highways. This allows the users of the matched log-normal model to choose these parameters considering the traffic density of their highway only, independent of the highway they are using for their simulation.

To validate the proposed matched log-normal model, we have extended the simulations for various vehicle traffic densities and three additional highway roads I5-S, I80-E and I580-W in California, and checked the agreement of the resulting matched parameters including path loss exponent, standard deviation and correlation factor for matched log-normal model on these highway roads. The realistic mobility over the additional roads is generated by determining the input and parameters of the microscopic mobility

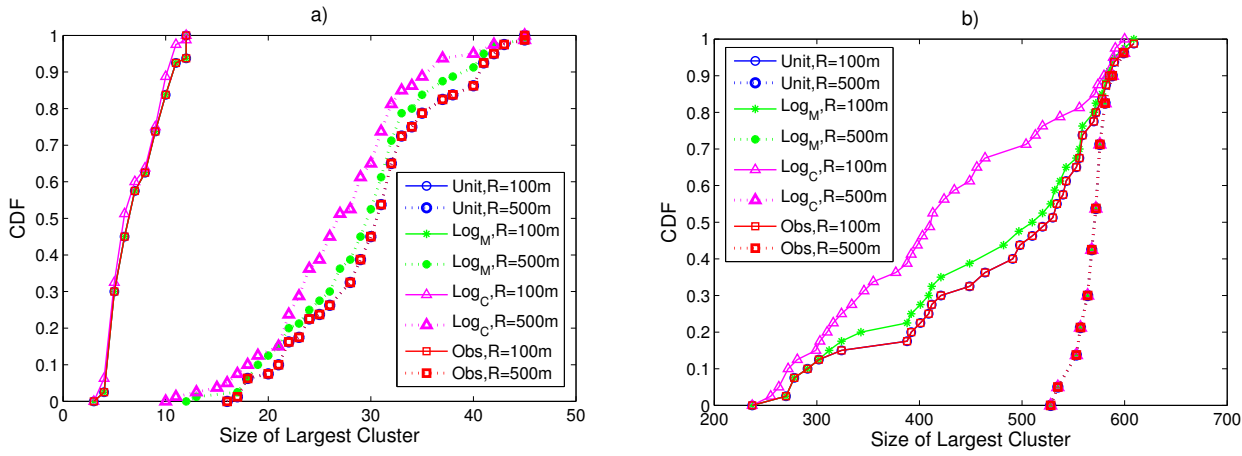


Fig. 12: Cdf of the size of the largest cluster metric for different channel models and transmission ranges in a) low density and b) high density networks

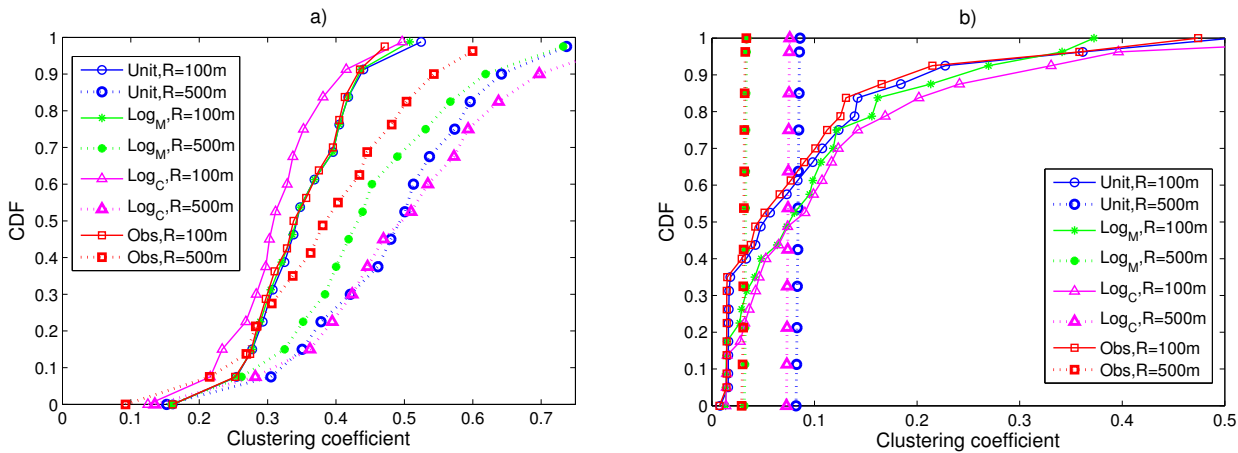


Fig. 13: Cdf of the clustering coefficient metric for different channel models and transmission ranges in a) low density and b) high density networks

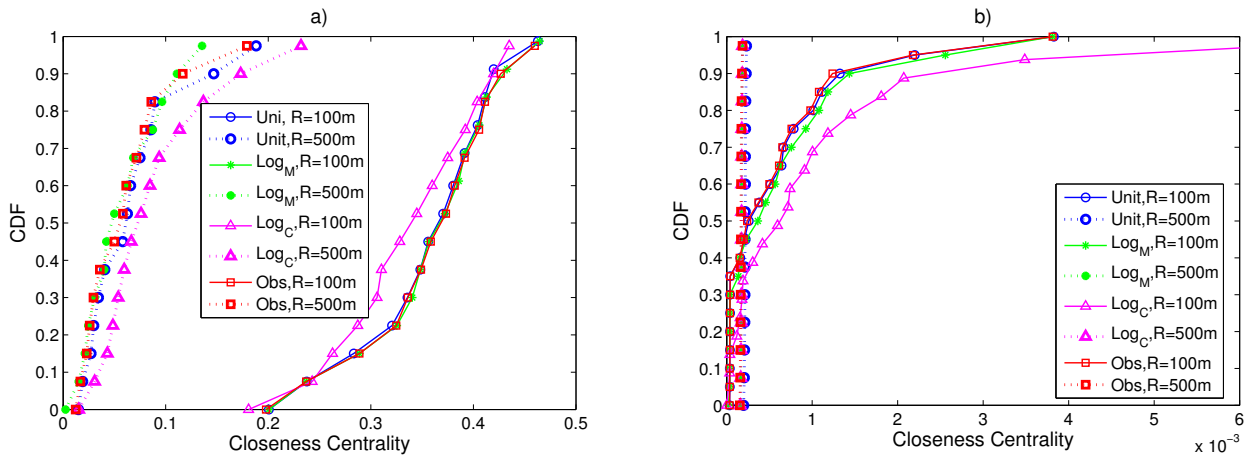


Fig. 14: Cdf of the closeness centrality metric for different channel models and transmission ranges in a) low density and b) high density networks

simulator SUMO based on the flow and speed information provided by the PeMS database as explained in detail in Section III. The vehicle mobility output of SUMO is then input to MATLAB where the values of the path loss exponent, standard deviation and correlation factor that provide the best match to the obstacle based model are determined. These roads are chosen such that they are different in vehicle traffic density, the number of lanes and

intersections.

Figs. 15, 16 and 17 show the matched path loss exponent, standard deviation and correlation factor values respectively for I880-S, I5-S, I80-E and I580-W highway roads at different vehicle traffic densities and transmission ranges. We observe that the matched values of these parameters are consistent across different highways at different vehicle traffic densities and different trans-

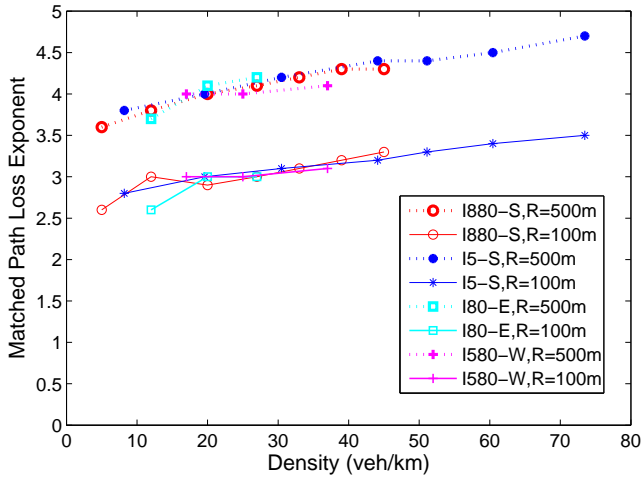


Fig. 15: Matched path loss exponent for I880-S, I5-S, I80-E and I580-W highway roads at different vehicle traffic densities and transmission ranges.

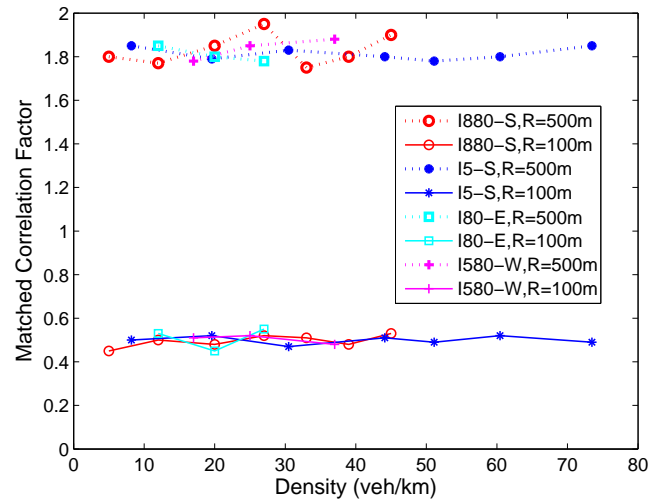


Fig. 17: Matched correlation factor for I880-S, I5-S, I80-E and I580-W highway roads at different vehicle traffic densities and transmission ranges.

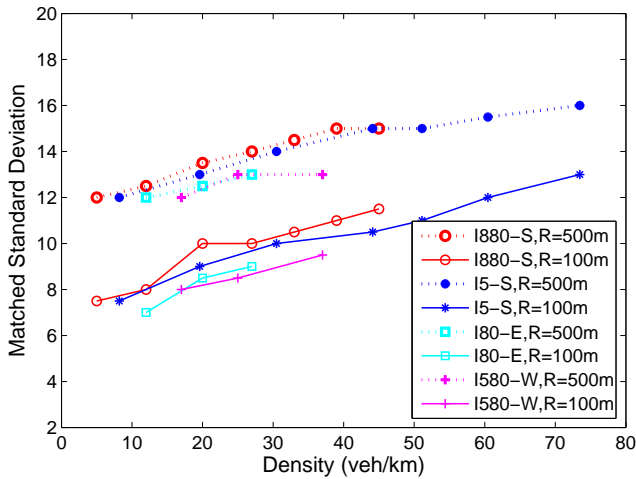


Fig. 16: Matched standard deviation for I880-S, I5-S, I80-E and I580-W highway roads at different vehicle traffic densities and transmission ranges.

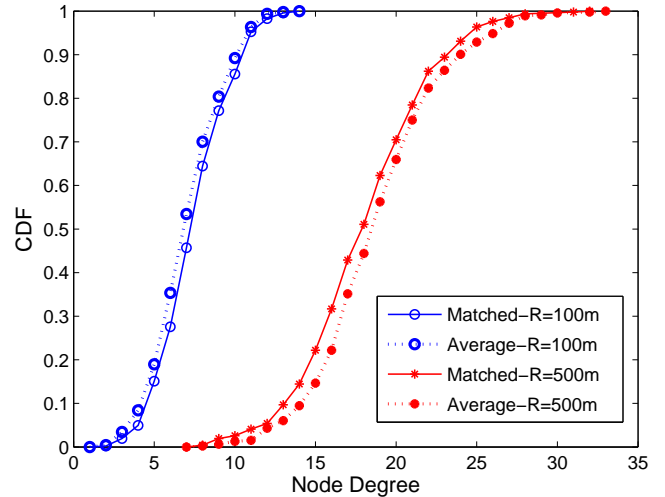


Fig. 18: Cdf of the node degree obtained by matching to the obstacle based model and using the matched parameters averaged over several roads on I580-W at high vehicle traffic density.

mission ranges.

We have further validated the dependency of the matched parameters on the traffic density by checking the agreement between the cdf of the performance metrics obtained by matching to the obstacle based model and using the matched parameters averaged over several roads. As an example, Figs. 18 and 19 show the cdf of the node degree and link duration on I580-W at high vehicle traffic density respectively. We observe good agreement of the cdfs.

## IX. CONCLUSION

We analyze the spatial and temporal evolution of the VANET topology characteristics by using both realistic large-scale mobility traces and realistic channel models. The realistic large-scale mobility traces are obtained by using accurate microscopic mobility modeling of SUMO, determining its input and parameters based on the vehicle flow and speed data extracted from the PeMS database. The realistic channel model is obtained by implementing a recently proposed obstacle based channel model that takes all

the vehicles around the transmitter and receiver into account in determining the received signal strength. The performance of the obstacle based model is compared to the most commonly used and more simplistic channel models including unit disc and log-normal shadowing models.

The extensive investigation of the system metrics regarding the link characteristics over both time and space including node degree, neighbor distance distribution, number of clusters and link duration reveals that tuning the parameters appropriately and introducing time correlation for the Gaussian random variable in the log-normal model provides a good match with the more sophisticated and computationally expensive obstacle based model. We validate the dependency of the values of these parameters on the vehicle traffic density only based on the real data of four different highways in California.

As future work, we plan to extend the proposed realistic simu-

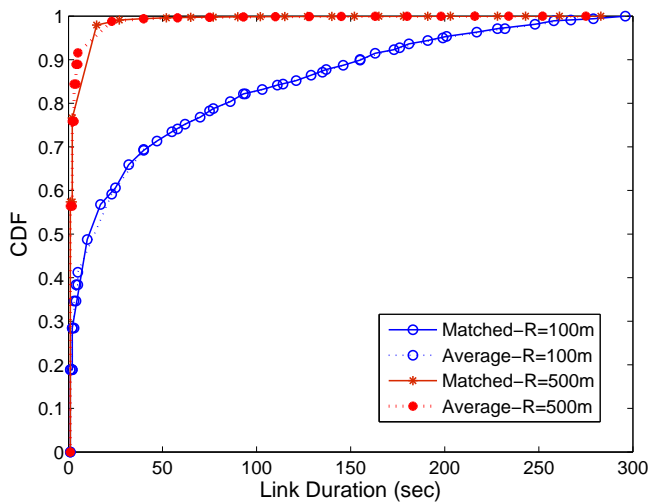


Fig. 19: Cdf of the link duration obtained by matching to the obstacle based model and using the matched parameters averaged over several roads on I580-W at high vehicle traffic density.

lation model and matching mechanism for urban traffic scenarios.

#### REFERENCES

- [1] N. Akhtar, O. Ozkasap, and S. Ergen, "Vanet topology characteristics under realistic mobility and channel models," in *IEEE Wireless Communication and Networking Conference (WCNC)*, April 2013, pp. 1774 – 1779.
- [2] R. Chen, W.-L. Jin, and A. Regan, "Broadcasting safety information in vehicular networks: issues and approaches," *IEEE Network*, vol. 24, no. 1, pp. 20–25, Jan-Feb 2010.
- [3] W. Chen and S. Cai, "Ad hoc peer-to-peer network architecture for vehicle safety communications," *IEEE Communications Magazine*, vol. 43, no. 4, pp. 100 – 107, April 2005.
- [4] M. Torrent-Moreno, J. Mittag, P. Santi, and H. Hartenstein, "Vehicle-to-vehicle communication: Fair transmit power control for safety-critical information," *IEEE Transactions on Vehicular Technology*, vol. 58, no. 7, pp. 3684 – 3703, September 2009.
- [5] J. Nzouonta, N. Rajgure, G. Wang, and C. Borcea, "Vanet routing on city roads using real-time vehicular traffic information," *IEEE Transactions on Vehicular Technology*, vol. 58, no. 7, pp. 3609 – 3626, September 2009.
- [6] Y. Toor, P. Muhlethaler, and A. Laouiti, "Vehicle ad hoc networks: applications and related technical issues," *IEEE Communications Surveys Tutorials*, vol. 10, no. 3, pp. 74 – 88, Third Quarter 2008.
- [7] S. A. H. Tabatabaei, M. Fleury, N. N. Qadri, and M. Ghanbari, "Improving propagation modeling in urban environments for vehicular ad hoc networks," *IEEE Transactions on Intelligent Transportation Systems*, vol. 12, no. 3, pp. 705 – 716, September 2011.
- [8] D. Dhoutaut, A. Régis, and F. Spies, "Impact of radio propagation models in vehicular ad hoc networks simulations," in *Proceedings of the 3rd international workshop on Vehicular ad hoc networks (VANET)*, September 2006, pp. 40–49.
- [9] S. Uppoor and M. Fiore, "Large-scale urban vehicular mobility for networking research," in *IEEE Vehicular Networking Conference (VNC)*, November 2011, pp. 62–69.
- [10] Tapascologne project. [Online]. Available: <http://sourceforge.net/apps/mediawiki/sumo/index.php?title=TAPASCologne>
- [11] D. Naboulsi and M. Fiore, "On the instantaneous topology of a large-scale urban vehicular network: the cologne case," in *ACM International Symposium on Mobile Ad Hoc Networking and Computing (MobiHoc)*, July 2013, pp. 1–9.
- [12] G. Pallis, D. Katsaros, M. D. Dikaiados, N. Loulloudes, and L. Tassioulas, "On the structure and evolution of vehicular networks," in *Modeling, Analysis and Simulation of Computer and Telecommunication Systems (MASCOTS)*, September 2009, pp. 1–10.
- [13] V. Naumov, R. Baumann, and T. Gross, "An evaluation of inter-vehicle ad hoc networks based on realistic vehicular traces," in *Proceedings of the 7th ACM international symposium on Mobile ad hoc networking and computing (MobiHoc)*, May 2006, pp. 108–119.
- [14] M. Boban, W. Viriyasitavat, and O. Tonguz, "Modeling vehicle-to-vehicle line of sight channels and its impact on application-layer performance," in *Proceedings of the tenth ACM international workshop on Vehicular inter-networking, systems, and applications*, ser. VANET '13. New York, NY, USA: ACM, 2013.

- [15] Drive-in (distributed routing and infotainment through vehicular inter-networking). [Online]. Available: <http://drive-in.cmuportugal.org>
- [16] W. Viriyasitavat, F. Bai, and O. K. Tonguz, "Dynamics of network connectivity in urban vehicular networks," *IEEE Journal on Selected Areas in Communications*, vol. 29, no. 3, pp. 515 – 533, March 2011.
- [17] M. Fiore and J. Harri, "The networking shape of vehicular mobility," in *ACM International Symposium on Mobile Ad hoc Networking and Computing (MobiHoc)*, May 2008, pp. 261–272.
- [18] R. Meireles, M. Ferreira, and J. Barros, "Vehicular connectivity models: From single-hop links to large-scale behavior," in *IEEE Vehicular Technology Conference (VTC) Fall*, September 2009, pp. 1–5.
- [19] R. Protzmann, B. Schunemann, and I. Radosch, "The influences of communication models on the simulated effectiveness of  $\sqrt{2x}$  applications," *IEEE Communications Magazine*, vol. 49, no. 11, pp. 149 – 155, November 2011.
- [20] S. C. Ng, W. Zhang, Y. Zhang, Y. Yang, and G. Mao, "Analysis of access and connectivity probabilities in vehicular relay networks," *IEEE Journal on Selected Areas in Communications*, vol. 29, no. 1, pp. 140 – 150, January 2011.
- [21] X. Jin, W. Su, and Y. Wei, "Quantitative analysis of the vanet connectivity: Theory and application," in *IEEE Vehicular Technology Conference (VTC) Spring*, May 2011, pp. 1–5.
- [22] J. Gozalvez, M. Sepulcre, and R. Bauza, "Impact of the radio channel modelling on the performance of vanet communication protocols," *Telecommunication Systems*, pp. 1–19, December 2010.
- [23] Performance measurement system (PeMS). [Online]. Available: <http://pems.dot.ca.gov/>
- [24] SUMO - Simulation of Urban MObility. [Online]. Available: <http://sumo.sourceforge.net>
- [25] J. Harri, F. Filali, and C. Bonnet, "Mobility models for vehicular ad hoc networks: A survey and taxonomy," *IEEE Communications Surveys and Tutorials*, vol. 11, no. 4, pp. 19 – 41, Fourth Quarter 2009.
- [26] Vissim. [Online]. Available: [http://www.english.ptv.de/cgi-bin/traffic/traf\\_vissim.pl](http://www.english.ptv.de/cgi-bin/traffic/traf_vissim.pl)
- [27] H. Conceicao, L. Damas, M. Ferreira, and J. Barros, "Large scale simulation of v2v environments," in *ACM Symposium on Applied Computing*, March 2008, pp. 28–33.
- [28] B. Raney, A. Voellmy, N. Cetin, M. Vrtic, and K. Nagel, "Towards a microscopic traffic simulation of all of switzerland," in *International Conference on Computational Science*, April 2002, pp. 371–380.
- [29] J. Maurer, T. Fugen, M. Porebska, T. Zwick, and W. Wiesbeck, "A ray-optical channel model for mobile to mobile communications," in *4th MCM COST 2100*, February 2008.
- [30] C. F. Mecklenbrauker, A. F. Molisch, J. Karedal, F. Tufvesson, A. Paier, L. Bernardo, T. Zemen, O. Klemp, and N. Czink, "Vehicular channel characterization and its implications for wireless system design and performance," *Proceedings of the IEEE*, vol. 99, no. 7, pp. 1189 – 1212, July 2011.
- [31] J. Karedal, N. Czink, A. Paier, F. Tufvesson, and A. F. Molisch, "Path loss modeling for vehicle-to-vehicle communications," *IEEE Transactions on Vehicular Technology*, vol. 60, no. 1, pp. 323 – 328, January 2011.
- [32] L. Cheng, B. E. Henty, F. Bai, and D. D. Stancil, "Highway and rural propagation channel modeling for vehicle-to-vehicle communications at 5.9 ghz," in *IEEE Antennas and Propagation Society International Symposium*, July 2008, pp. 1–4.
- [33] G. Setiawan, S. Iskandar, S. Kanhere, and K. chan Lan, "The effect of radio models on vehicular network simulations," October 2007.
- [34] L. Cheng, B. E. Henty, D. D. Stancil, F. Bai, and P. Mudalige, "Mobile vehicle-to-vehicle narrow-band channel measurement and characterization of the 5.9 ghz dedicated short range communication (dsrc) frequency band," *IEEE Journal on Selected Areas in Communications*, vol. 25, no. 8, pp. 1501 – 1516, October 2007.
- [35] O. Renaudin, V.-M. Kolmonen, P. Vainikainen, and C. Oestges, "Non-stationary narrowband mimo inter-vehicle channel characterization in the 5-ghz band," *IEEE Transactions on Vehicular Technology*, vol. 59, no. 4, pp. 2007 – 2015, May 2010.
- [36] M. Boban, T. T. V. Vinhoza, M. Ferreira, J. Barros, and O. K. Tonguz, "Impact of vehicles as obstacles in vehicular ad hoc networks," *IEEE Journal on Selected Areas in Communications*, vol. 29, no. 1, pp. 15 – 28, January 2011.
- [37] J. Karedal, F. Tufvesson, N. Czink, A. Paier, C. Dumard, T. Zemen, C. F. Mecklenbrauker, and A. F. Molisch, "A geometry-based stochastic mimo model for vehicle-to-vehicle communications," *IEEE Transactions on Wireless Communications*, vol. 8, no. 7, pp. 3646 – 3657, July 2009.
- [38] J. Maurer, T. Fugen, and W. Wiesbeck, "Narrow-band measurement and analysis of the inter-vehicle transmission channel at 5.2 ghz," in *IEEE Vehicular Technology Conference (VTC) Spring*, May 2002, pp. 1274–1278.
- [39] I. Sen and D. Matolak, "Vehicle-to-vehicle channel models for the 5-ghz band," *IEEE Transactions on Intelligent Transportation Systems*, vol. 9, no. 2, pp. 235 – 245, June 2008.
- [40] D. Krajzewicz, M. Bonert, and P. Wagner, "The open source traffic simulation package sumo," in *RoboCup Infrastructure Simulation Competition*, June 2006, pp. 371–380.

- [41] J. Epstein and D. Peterson, "An experimental study of wave propagation at 850 mc," *Proceedings of the IRE*, vol. 41, no. 5, pp. 595–611, May 1953.
- [42] J. Deygout, "Multiple knife-edge diffraction of microwaves," *IEEE Transactions on Antennas and Propagation*, vol. 14, no. 4, pp. 480–489, July 1966.
- [43] C. Giovaneli, "An analysis of simplified solutions for multiple knife-edge diffraction," *IEEE Transactions on Antennas and Propagation*, vol. 32, no. 3, pp. 297–301, March 1984.
- [44] "Propagation by diffraction," *International Telecommunication Union Radio-communications Sector, Geneva*, p. P.526, February 2007.
- [45] M. Gudmundson, "Correlation model for shadow fading in mobile radio systems," *Electronics Letters*, vol. 27, no. 23, pp. 2145–2146, 1991.
- [46] J. Gozalvez, M. Sepulcre, and R. Bauza, "Impact of the radio channel modelling on the performance of vanet communication protocols," *Telecommunication Systems*, vol. 50, no. 3, pp. 149–167, 2012.
- [47] M. Sepulcre and J. Gozalvez, "Adaptive wireless vehicular communication techniques under correlated radio channels," in *IEEE Vehicular Technology Conference (VTC) Spring*, April 2009, pp. 1–5.
- [48] S. Szyszkowicz, H. Yanikomeroglu, and J. Thompson, "On the feasibility of wireless shadowing correlation models," *IEEE Transactions on Vehicular Technology*, vol. 59, no. 9, pp. 4222–4236, November 2010.
- [49] Data sets of vehicle mobility and communication channel models for realistic and efficient vanet highway simulation. [Online]. Available: [http://cs-people.bu.edu/nabee1/VANETs\\_Mobility\\_Dataset/](http://cs-people.bu.edu/nabee1/VANETs_Mobility_Dataset/)